

# A Search for Beyond Standard Model Physics from

$$p\bar{p} \rightarrow ZX \rightarrow e^+e^-X \text{ at FNAL}$$

Fred Niell

8/02

Preliminary Defense for Candidacy

## Abstract

Many beyond Standard Model (SM) theories posit the existence of a new neutral gauge boson, the  $Z'$ , in addition to the panoply of SM particles. While there has yet to be unequivocal evidence for or against such a particle, many theories rely on this newly introduced particle. As a result, searches for this new boson provide a window into physics outside the SM realm. This paper presents the status and mechanics of one such search, some of the beyond-SM theories to be studied, and some preliminary results.

## 1 Introduction

Truly successful grand unification theories (GUT)s have been eluding physicists since the first attempt to unite the strong, weak, gravitational and electromagnetic forces nearly a century ago. While no particular GUT seems likely as an explanation of nature, several have been shown to be consistent with experimental data. In particular, GUTs that involve

making the  $SU(3) \times SU(2) \times U(1)$  group (which accurately describes the standard model (SM)) a subgroup of a larger symmetry group have been quite successful. Even GUT schemes involving more exotic group theoretical techniques have shown promise. One consequence of several of these theories is the existence of new neutral gauge bosons, typically referred to as  $Z'$  bosons. Generally speaking, these new gauge bosons are similar to the SM  $Z$  (which we will denote as  $Z_0$  for clarity). Detection efforts for these new bosons are currently under way. One means of detecting a  $Z'$  is to examine the  $A_{FB}$  for Drell Yan dilepton pair production from  $p\bar{p}$  collisions, i.e.  $p\bar{p} \rightarrow Z' + (X) \rightarrow \ell\bar{\ell} + (X)$ .

In this paper I will present the methods used to investigate the  $A_{FB}$ , some theoretical motivations, and a few preliminary results. Measurement of the  $A_{FB}$  involves first creating a large sample of dilepton events, properly chosen to include the  $Z_0$  pole and as many high-mass limit events as possible. Using the Collider Detector at Fermilab (CDF), dilepton data is collected and analyzed, using algorithms developed to efficiently cull the dileptons from the myriad other events. From there, the leptons' momenta are transposed into the Collins-Soper [17] frame to minimize ambiguity in the momentum introduced by the initial state parton transverse momentum ( $P_t$ ). From the leptons' presence in either the positive or negative hemisphere of this frame, plus simple calculation, the  $A_{FB}$  for the event is established. The  $A_{FB}$  for each event will then be studied with respect to invariant mass of the lepton pair. Inconsistencies with the SM show up in the departure from  $A_{FB} = 0.6$  in the high mass limit, in accordance with the beyond-SM models to be presented. [14, 16]

## 2 The $A_{FB}$ Asymmetry

### *Calculating the $A_{FB}$*

Dilepton production, i.e.  $p\bar{p} \rightarrow \ell\bar{\ell}$  is mediated by virtual photons, the SM  $Z_0$ , and photon- $Z$  interference, depending on the mass of the dilepton pair. Below the  $Z_0$  mass, the reaction is mediated by a virtual photon exchange. In the neighborhood of the  $Z_0$  mass (91 GeV), the  $Z_0$  boson mediates. And above the  $Z_0$  mass,  $Z$ -photon (called  $Z/\gamma$  interference) reigns. In the process  $q\bar{q} \rightarrow Z/\gamma \rightarrow \ell\bar{\ell}$ , the bosons have both vector and axial vector couplings to the fermions. These couplings create an asymmetry in the momentum of the electron, visible in the polar angle of the lepton pair's center of mass frame. This polar angle measured in the center of mass frame of the leptons is typically referred to as the Collins Soper frame [17].

The angular cross section measured in this frame is given by

$$\frac{d\sigma(q\bar{q} \rightarrow Z/\gamma \rightarrow \ell\bar{\ell})}{d\cos(\theta^*)} = A(1 - \cos^2(\theta^*)) + B \cos(\theta^*) \quad (1)$$

calculated to tree level only. Here,  $\theta^*$  is the emission angle of the electron relative to the quark momentum in the leptons' center of mass frame. The constants  $A$  and  $B$  are determined by the weak isospin and charge of the incident quarks as well as the mass of the dilepton pair. From this cross section, it is convenient to define  $N_f$  as the number of events whose  $\theta^*$  is positive, and  $N_b$  as the number of events whose  $\theta^*$  is negative. The asymmetry can then be written

$$A_{FB} = \frac{\left(\frac{d\sigma}{d\cos(\theta^*)_{>0}}\right) - \left(\frac{d\sigma}{d\cos(\theta^*)_{<0}}\right)}{\left(\frac{d\sigma}{d\cos(\theta^*)_{>0}}\right) + \left(\frac{d\sigma}{d\cos(\theta^*)_{<0}}\right)}$$

$$\begin{aligned}
&= \frac{3}{8} \times \frac{B}{A} \\
&= \frac{N_f - N_b}{N_f + N_b}
\end{aligned} \tag{2}$$

Of course, this is neglecting a number of important factors, but this is the general form of the asymmetry.

### *Kinematics of $\cos(\theta^*)$*

Collins and Soper [17] noted that an ambiguity exists in the determination of the emission angle  $\theta^*$  when considering  $q\bar{q} \rightarrow \ell\bar{\ell}$ . This Drell-Yan process is quite simple when the incoming quarks have no transverse momentum. In such a case, the emission angle is determined by the angle the electron makes with the proton beam, and thus the incoming quark momentum vector. However, since circular acceleration implies a certain amount of transverse momentum by construction, an ambiguity arises. Since the quarks' individual momenta can not be measured, the momenta boosted into the center of mass frame of the leptons are even more difficult to separate. Consequently, the dependence of the transverse momentum must be minimized. The Collins Soper formalism does so with the following prescription,

$$\cos(\theta^*) = \frac{2(l_1^+ l_2^- - l_1^- l_2^+)}{M \sqrt{M^2 + P_T^2}} \tag{3}$$

Here we have labeled  $l_{1,2}^{(+,-)}$  the (1) electron and (2) positron. The  $l^{(+,-)}$  nomenclature represents the following:

$$\begin{aligned}
l^{(+,-)} &= \frac{1}{\sqrt{2}} (p^0 \pm p^3) \\
\vec{P} &= [p^0 \equiv E, p^1, p^2, p^3]
\end{aligned} \tag{4}$$

Where the  $\vec{\mathcal{P}}$  is the 4-momentum of the lepton,  $p^3$  the longitudinal component of the lepton momentum. The polar ( $\theta^*$ ) axis is the bisector of the proton beam momentum and the negative ( $-$ ) of the antiproton beam momentum when the two are boosted into the center of mass frame of the leptons. In so doing, the dependence on the transverse momentum of the incoming quark pair is minimized. Figure 1 shows the kinematics of the frame's calculation. In the upper half (1), the leptons' center of mass frame is shown. The lower half of the figure shows the bisector-determined z axis, and the leptons' new relative emission angle.

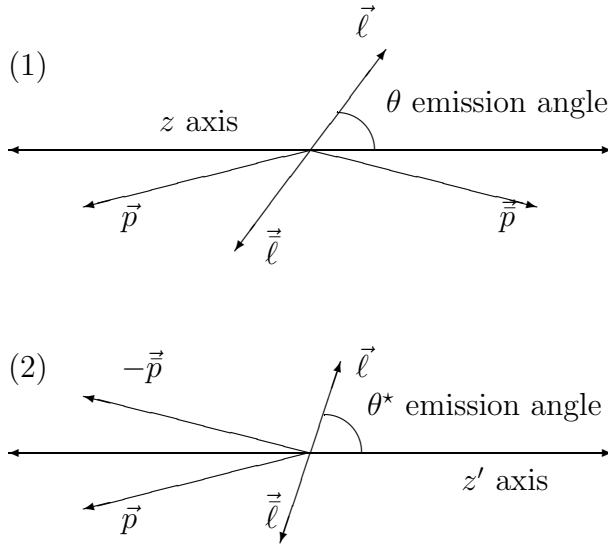


Figure 1: Kinematics of (1) center of mass frame of leptons, and (2) the Collins-Soper frame

Generally speaking, standard model predicts that the  $A_{FB}$  should approach  $-50\%$  for  $M_{\ell\ell} \leq M_{Z_0}$ ,  $\approx 0\%$  at  $M_{\ell\ell} \approx M_{Z_0}$ , and  $+50\%$  for  $M_{\ell\ell} \geq M_{Z_0}$ . Monte Carlo studies give very good estimates for the value of the  $A_{FB}$  with sufficient statistics. By way of demonstration, a sample  $\cos(\theta^*)$  histogram is presented in Figure 2 for a few certain  $Z$  candidates whose mass is near the  $Z_0$  mass of  $91.2 \frac{\text{GeV}}{c^2}$ . Same sign background events are shown in red in this sample. Note that in this particular mass bin, there appear to be more or less equal numbers

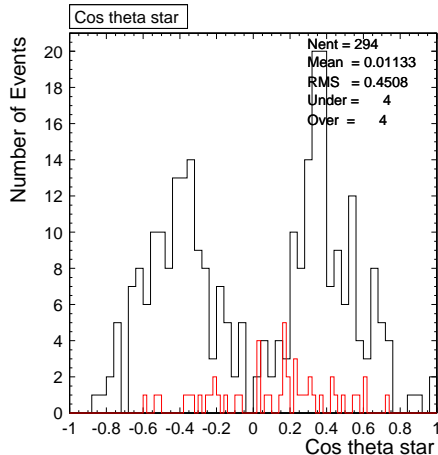


Figure 2:  $\cos(\theta^*)$  for CP  $Z$  candidates whose mass  $\in [75, 105]$

of events whose  $\cos(\theta^*)$  is above 0 as below. Numerical analysis indeed shows that the  $A_{FB}$  for this bin is  $\approx +0.01$  which is in line with the SM prediction.

### 3 $Z \rightarrow \ell^+ \ell^-$ sample selection

#### *Event Selection*

Historically, the most difficult aspect of this particular analysis is the event selection. At CDF, many events can mask themselves as leptons, and many leptons can disguise themselves as other particles. For that reason, sophisticated algorithms are currently being devised to aid in the selection of dilepton events. The Electron Task Force at Fermilab is in charge of determining the correct cuts utilized in the selection of leptons. The current form of this analysis uses the cuts defined by the electron task force. Each  $Z$  is characterized by two electrons. Events with at least one “tight” electron and at least one “loose” electron are called a Central-Central (CC)  $Z$  candidate. Events with one “tight” electron and at least

one plug electron are defined as Central-Plug (CP)  $Z$  candidates. Note that in Table 1 the last entry is the Track Q, or the relative track charges. The “tight” charge times the “loose” charge must be negative, ensuring that whichever one is negative, the two tracks have opposite charge. A summary of the values of these cuts for CC  $Z$  candidates is shown in Table 1 and for CP  $Z$  candidates in Table 2.

### *Electron Variables*

Variables used in the selection of the electrons for this analysis are shown in Tables 1 and 2. These variables are chosen specifically for their selection power and insensitivity to backgrounds. In Figure 3 each of the following variables’ shapes are plotted for their associated electron candidates. The resulting invariant masses are plotted in Figure 4.

- $E_T$ : Transverse Electromagnetic Energy

Within the detector, electromagnetic clusters are identified by a seed EM tower and shoulder EM towers. The size of the cluster is restricted to  $\Delta\eta \leq 0.3$  and  $\Delta\phi \leq 15^\circ$ . From the cluster, the transverse component of the EM energy,  $E_T$ , is calculated ( $E_T = E_{cluster} \sin\theta$  with  $\theta$  measured by the COT track associated with the electron).

- Had/EM: Ratio of Hadronic to Electromagnetic Energy

Defined as the ratio of total hadron calorimeter energy to the total EM calorimeter energy for the EM cluster of the associated electron.

- $E_T^{iso}/E_T^{electron}$ : Isolation  $E_T$  fraction in a cone of  $R = 0.4$

The isolation  $E_T$  for an EM cluster is the total  $E_T$  within a cone in  $\eta - \phi$  space with a radius of  $R=0.4$  excluding the tower itself. The radius is defined as  $\Delta R = \sqrt{\Delta\eta^2 + \Delta\phi^2}$  for  $\Delta R$  between the cluster centroid and the candidate tower center. The fraction is defined as  $E_T^{iso}/(E_T^{iso} - E_T^{electron})$ .

- $\chi_{strip}^2$ :  $\chi^2$  fit to test beam

CES pulse height and shapes are compared to test beam data with a  $\chi^2$  fit to determine the event’s energy signature likeness to test beam. The variable is the fit of the energy deposited in each of the 11 strips in  $z$  in the CES shower to test beam data.

- $L_{shr}$ : Transverse energy sharing

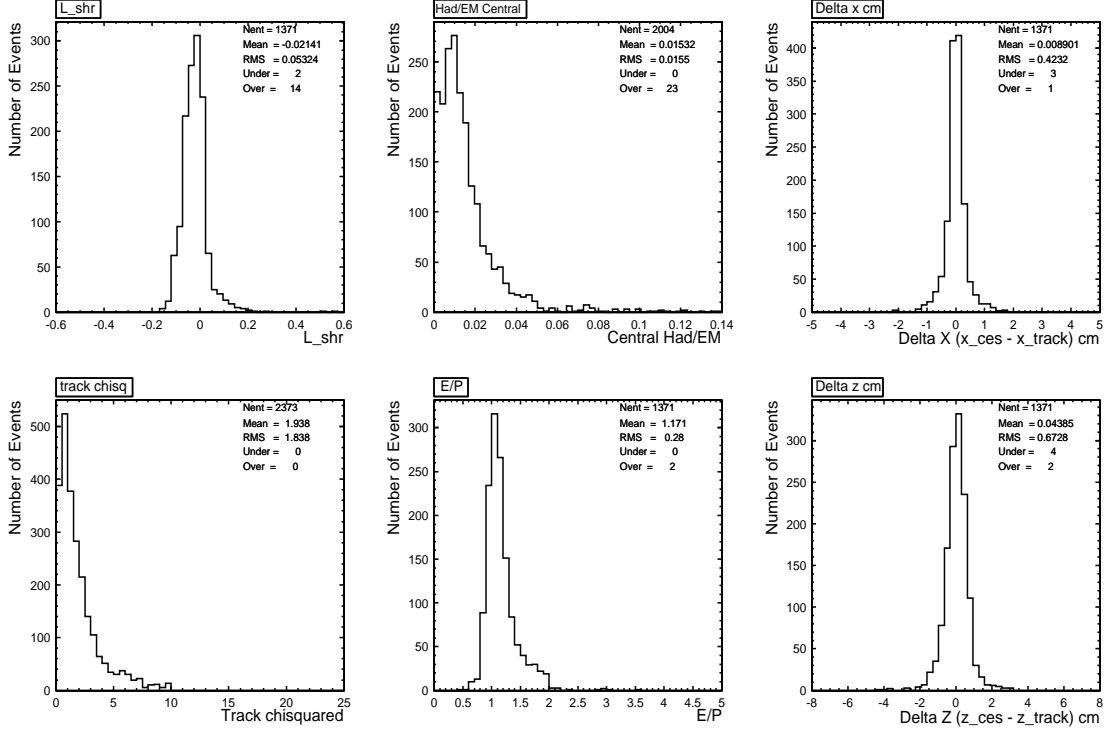


Figure 3: Clockwise from top left,  $L_{shr}$ , Had/EM, track  $\chi^2$ ,  $\Delta Z$ , E/P,  $\Delta X$

Transverse profiles of electrons are measured, giving a comparison of the lateral energy sharing in calorimeter towers of an EM cluster to test beam EM clusters.  $L_{shr}$  is defined by

$$L_{shr} = 0.14 \times \sum_i \frac{E_i^{adj} - E_i^{expected}}{\sqrt{(0.14\sqrt{E})^2 + (\Delta E_i^{expected})^2}} \quad (5)$$

for  $E_i^{adj}$  is the measured tower energy,  $E_i^{expected}$  the test beam data,  $0.14\sqrt{E}$  the energy measurement error, and  $\Delta E_i^{expected}$  the error in the test beam data.

- $E/P$  and  $P_T$ : Ratio of EM energy to momentum

Tracks are defined as the highest  $P_T$  COT track pointing to the electron EM cluster.  $E/P$  is the ratio of the calorimeter determined EM energy to the COT measured momentum. Note the long tail on  $E/P$ . This is due to electrons passing through the inner wall of the COT and producing *bremsstrahlung* radiation. The COT's measurement of  $\vec{P}$  is smaller than the calorimeter, as it doesn't pick up the collinear photons created in the *bremsstrahlung* process. The calorimeter, however, picks up the extra photons as they generally land in the same calorimeter cell as the electron.

- $Z_{vertex}$ : Interaction point in  $z$ , measured by COT track extrapolation
- $\Delta X$  and  $\Delta Z$ :  $\Delta X = r - \phi$  separation,  $\Delta Z = z$  separation

- Fiduciality: Is the electron in the fiducial detector volume? The fiduciality is determined by the detector’s electronics interfacing the Hardware Database, which stores test beam data information and position calibrations.

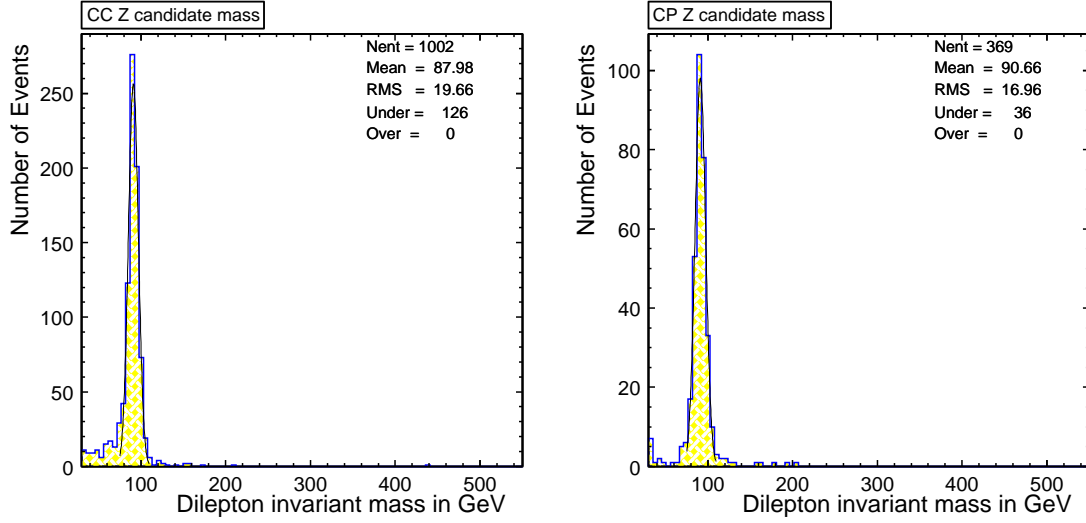


Figure 4: CP, CC candidate events invariant mass Z-peaks around  $M= 91.2\text{GeV}$ , some high mass events

Cut Variable	Central “Tight” electron	Central “Loose” electron
$E_T^{corrected}$	$\geq 25 \text{ GeV}$	$\geq 25 \text{ GeV}$
$\eta$	$\leq 1.0$	$\leq 1.0$
Had/EM	$< 0.05$	$< 0.05$
$E_T^{iso}/E_T^{electron}$	$< 0.1$	$< 0.1$
$P_T$	$0.5 < E_T^{corrected}/P < 2$	$P_T \geq 10 \text{ GeV}$
$Z_{vertex}$	$ z_0^{electron}  \leq 60\text{cm}$	—
$L_{shr}$	$< 0.2$	—
$\chi_{strip}^2$	$< 10$	—
$ \Delta X $	$< 1.5 \text{ cm}$	—
$ \Delta Z $	$< 3 \text{ cm}$	—
Track Q	$Q_{tight} \times Q_{loose} < 0$	

Table 1: Electron Task Force electron cuts for Central-Central Z’s

The invariant mass is calculated by determining the emission angle between the two leptons in the detector’s coordinate system to determine the momenta of the leptons. The

Cut Variable	Central “Tight” electron	Plug electron
$E_T^{corrected}$	$\geq 25$ GeV	$\geq 25$ GeV
$\eta$	$\leq 1.0$	$1 <  \eta  \leq 3$
Had/EM	$< 0.05$	$< 0.05$
$E_T^{iso}/E_T^{electron}$	$< 0.1$	$< 0.1$
$P_T$	$0.5 < E^{corrected}/P < 2$	—
$Z_{vertex}$	$ z_0^{electron}  \leq 60\text{cm}$	—
$L_{shr}$	$< 0.2$	—
$\chi_{strip}^2$	$< 10$	—
$ \Delta X $	$< 1.5$ cm	—
$ \Delta Z $	$< 3$ cm	—

Table 2: Electron Task Force electron cuts for Central-Plug Z’s

invariant mass is the combined mass of the two particles in the center of mass frame. A simple 2-body decay system is a perfect example. The emission angle between the two decay particles is defined as  $\alpha$ . Using the simple assumption that at high energy,  $E \simeq p$  and  $m_{1,2} \ll s$ , the mass is given as such:

$$\begin{aligned}
M^2 &= m_1^2 + m_2^2 + 2E_1E_2 - 2p_1p_2 \cos \alpha \\
M &= \sqrt{2(E_1E_2 - p_1p_2 \cos \alpha)} \\
&= \sqrt{2(E_1E_2(1 - \cos \alpha))} \tag{6}
\end{aligned}$$

Since the energies of the two particles is measured for the experimenter, all that remains to calculate the mass from Equation 6 is the opening angle between the two particles. Rather complicated angular subtraction algebra is needed. Since the particles’ azimuthal angle  $\phi$  is given, there is cause for relief. However, each leptons’ polar angle  $\theta$  is given in the Lorentz invariant pseudo rapidity nomenclature  $\eta$ , where  $\eta = \frac{1}{2} \ln \frac{p_{\perp} - p_{\parallel}}{p_{\perp} + p_{\parallel}}$  [18]. The  $\eta$  is related to the lab frame polar angle  $\theta$  by  $\eta = -\ln\left(\tan\left(\frac{\theta}{2}\right)\right)$ . Thus, to recover the polar angle, the following

relation is used,

$$\theta = 2 \arctan(e^{-\eta}) \quad (7)$$

This leads to the inevitable opening angle calculation [19] for leptons  $l_1$  and  $l_2$ ;

$$\alpha_{l\Delta l} = \frac{\cos(\phi_1 - \phi_2) + 4 \cot\left(\arctan(e^{-\eta_1})\right) \cot\left(\arctan(e^{-\eta_2})\right)}{\sqrt{1 + \cot^2\left(\arctan(e^{-\eta_1})\right)} \times \sqrt{1 + \cot^2\left(\arctan(e^{-\eta_2})\right)}} \quad (8)$$

The invariant mass distribution for all of the dilepton pairs is easily calculable, given the proper programming environment. The  $Z$  candidates are shown in Figure 4. Here the CC and CP candidates are shown in histograms according to the mass of the dilepton pair. Note the Gaussian fits to each, which are centered around the  $Z_0$  pole.

### *Electron Cut Efficiencies*

In order to determine the relative electron cut and identification efficiencies, Monte Carlo studies must be carried out. Typically, many pseudo experiments are carried out to create a sample of electron events that are designed to fit within the simulation of the CDF detector. From there, a set of  $(N - 1)$  plots are created, which show the number of events passing all but one variable for each variable in the selection code. This allows for a variable-by-variable study of the predictive power of each variable, and the efficiency for each cut in the event filter. The  $(N - 1)$  set has yet to be created for this analysis.

Charge of the lepton pairs is crucial in the background studies. In the estimation of opposite-sign background events, prior analyses have used the background estimates used in the TOP analysis [14]. The  $e\mu$  rates are taken to be twice that of the  $ee$  rates for Central-Central electrons assuming equal acceptances and efficiencies for  $e\mu$  and  $ee$  events.

The  $e\mu$  rates are taken to be half that of  $ee$  rates for CP and CF electrons as well. From the background estimates used in the TOP analyses, estimates for the opposite-sign backgrounds in the  $ee$  analysis.

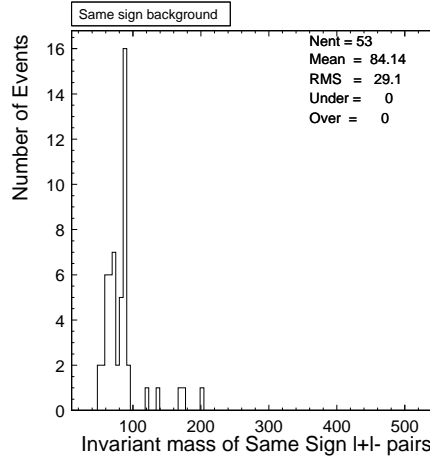


Figure 5: CC Same sign events, passing all but the opposite sign cut

Same-sign background events can arise from charge-symmetric QCD processes. These same-sign processes must be accounted for by measuring the isolation energy distribution of the dileptons. A recent analysis [14] used the isolation distributions measured in three mass regions;  $M_{ll} \approx (40 - 70, 70 - 105, 105 - \dots)\text{GeV}$ . The signal and background shapes for these regions were fit to the data, and an appropriate background subtraction scheme was utilized,

$$\left(\frac{d\sigma_i}{dM_i}\right)^{(+,-)} = \frac{(N_{events}^{(+,-)} - N_{background}^{(+,-)})_i}{\Delta M_i \left(\mathcal{L} \epsilon_i^{(+,-)} A_i^{(+,-)}\right)} \quad (9)$$

where the  $\mathcal{L}$  is the integrated luminosity,  $\epsilon_i$  is the combined detector efficiency, and the  $A_i$  is the calculated acceptance, and the index  $i$  represents the associated mass bin. James, *et al.* recently [21] published a study of the  $Z \rightarrow \mu\mu$  cross section for the CDF Run II data.

Their studies of acceptances and trigger efficiencies should prove a helpful guide.

In James' paper [21], the detector acceptance for  $W \rightarrow e\nu$  is measured to be  $A_{e\nu} = 0.15 \pm 0.05$ . This analysis finds a total of 56 same sign events that pass all but the charge cut. Since the actual values will require much more study, the present analysis will ignore the actual efficiency numbers until such time that they are more well understood.

## 4 Systematic and Statistical Uncertainties

The error propagation for this particular measurement proves to be relatively simple. Starting with Equation 9 and using the typical partial derivative uncertainty machinery,

$$\delta f(a_i) = \sqrt{\sum_i \left( \left. \frac{\partial f}{\partial a_i} \right|_{\bar{f}} \right)^2 \sigma_{a_i}^2} \quad (10)$$

we can calculate the uncertainty on the partial cross section. This assumes that each of the variables are independent and the errors are “small”, and cross terms in the variance propagation may be eliminated. Then we are left with the following equation

$$\delta\sigma_N = \left[ \left( \frac{-N_B\sigma_N}{\Delta M \mathcal{L} \epsilon A} \right)^2 + \left( \frac{N\sigma_{N_B}}{\Delta M \mathcal{L} \epsilon A} \right)^2 + \left( \frac{-(N + N_B)\sigma_{\Delta M}}{\Delta M^2 \mathcal{L} \epsilon A} \right)^2 + \left( \frac{-(N + N_B)\sigma_{\mathcal{L}}}{\Delta M \mathcal{L}^2 \epsilon A} \right)^2 + \left( \frac{-(N + N_B)\sigma_{\epsilon}}{\Delta M \mathcal{L} \epsilon^2 A} \right)^2 + \left( \frac{-(N + N_B)\sigma_A}{\Delta M \mathcal{L} \epsilon A^2} \right)^2 \right]^{\frac{1}{2}} \quad (11)$$

For the  $A_{FB}$  uncertainty is equally simple. Starting with Equation 2, and taking the proper derivatives,

$$\frac{\partial A_{FB}}{\partial \sigma_{N(\pm)}} = \pm \frac{2\sigma_{N(\pm)}}{(\sigma_{N+} + \sigma_{N-})^2} \quad (12)$$

$$\delta A_{FB} = \sqrt{\left[\frac{\partial A_{FB}}{\partial \sigma_{N+}}\right]^2 (\delta \sigma_{N+})^2 + \left[\frac{\partial A_{FB}}{\partial \sigma_{N-}}\right]^2 (\delta \sigma_{N-})^2} \quad (13)$$

The remaining piece of the puzzle is the uncertainty on  $\cos(\theta^*)$ . Equation 3 gives the relation for calculating the angle, however, the variables listed are not the explicit measurable quantities in the detector. The detector quantities are far more involved, and a somewhat simplified view will be presented. Since many of the detector-derived quantities have uncertainties already measured, such as  $M_T$ ,  $Q$ ,  $\Delta X$ , etc., their uncertainties will be taken for granted. Thus,

$$\begin{aligned} \cos(\theta^*) &\propto \frac{2E_t^2}{M\sqrt{M^2 + P_t^2}} \\ \delta \cos(\theta^*) &\simeq \sqrt{\left(\frac{4E\delta E}{M\sqrt{M^2 + P_t^2}}\right)^2 + \left(\frac{2E^2\delta M}{\sqrt{M^2 + P_t^2}}\right)^2 + \left(\frac{2E^2P_t\delta P_t}{M^3\sqrt{M^2 + P_t^2}}\right)^2} \\ &= \frac{2E}{M\sqrt{M^2 + P_t^2}} \sqrt{(ME\delta M)^2 + (2\delta E)^2 + (EP\sqrt{M^2 + P_t^2}\delta P_t)^2} \end{aligned} \quad (14)$$

which gives a reasonable estimate for the uncertainty on the  $\cos(\theta^*)$  measurement. Of course, this is assuming that the three variables  $M$ ,  $P_t$  and  $E_L$  are independent. Clearly, they are not. In fact, in the limit  $E \simeq p$ , all three are dependent on each other;  $P_t \equiv P \cos(\theta) \simeq E \cos(\theta)$ , and  $M = \sqrt{E^2(1 + \cos(\alpha))}$ . This will add to the uncertainty in the  $N_{\pm}$  and bring the naïve estimate beyond that of mere counting statistics.

## 5 Electroweak Theory, Consequences and Extensions

### *The SM Lagrangian and Neutral Current interactions*

Quantum field theory has shown us that from first principles, one can construct a Lagrangian utilizing various gauge groups that will behave like nature. Modern interpretations of field theory use a covariant derivative Lagrangian,

$$\mathcal{L}_{fermion} = \sum_f \bar{f} i \gamma^\mu \mathcal{D}_\mu f \quad (15)$$

with the covariant derivative  $\mathcal{D}_\mu$  being

$$\mathcal{D}_\mu = \partial_\mu - ig_1 \left( \frac{Y}{2} B_\mu \right)_Y - ig_2 \left( \frac{\tau^i}{2} W_\mu^i \right)_L - ig_3 \left( \frac{\lambda^a}{2} G_\mu^a \right)_Q \quad (16)$$

This Lagrangian gives us a description of nature that we have come to believe from a phenomenological standpoint in the field of particle physics. The second term in  $\mathcal{L}$  is the  $U(1)$  symmetry piece from hypercharge. The third term is the  $SU(2)$  group piece, giving us charged and neutral current interactions,  $W^{+-}$ ,  $Z_0$  bosons. The last term is the  $SU(3)$  group term, giving us the quark gluon interactions (the color charge piece). The  $g_{1,2,3}$  factors in front of the terms in the covariant derivative are the coupling strengths of the various interactions. [6, 5]

In this study the lepton  $U(1)$  term and the diagonal portion of the  $SU(2)$  are of particular importance, as they control the neutral current interactions. Starting with the lepton specific

interaction Lagrangian,

$$\mathcal{L} = \left( \bar{e}_L \gamma^\mu e_L + \bar{\nu}_L \gamma^\mu \nu_L \right) \left[ -\frac{g_1}{2} Y_L B_\mu + \frac{g_2}{2} W_\mu^\circ \right] + \bar{e}_R \gamma^\mu e_R \left[ -\frac{g_1}{2} Y_R B_\mu \right] \quad (17)$$

The neutrino should not have any electromagnetic interaction, so two orthogonal fields are defined;  $A_\mu$  and  $Z_\mu$ . The coefficient  $\bar{\nu}_L \gamma^\mu \nu_L$  must be the  $Z_\mu$  field, so that  $A_\mu$  and  $Z_\mu$  are orthogonal. Then the interaction Lagrangian becomes

$$\begin{aligned} \mathcal{L} &= -A_\mu \left( \bar{e}_L \gamma^\mu e_L Q_f + \bar{e}_R \gamma^\mu e_R Q_f \right) - Z_\mu \left( \bar{e}_L \gamma^\mu e_L Q_f + \bar{e}_R \gamma^\mu e_R Q_f \right); \\ &\text{for } Q_F \equiv T_3^f + \frac{Y_F}{2} \end{aligned} \quad (18)$$

The field  $Z_{mu}$  by construction contains vector and axial vector couplings, called  $V - A$  typically. This is easily seen from Dirac spinor identities [6];

$$\begin{aligned} \bar{\phi}_L \gamma^\mu \phi_L &= \frac{1}{2} \bar{\phi} \gamma^\mu (1 - \gamma^5) \phi \\ Z_\mu &= \bar{\nu}_L \gamma^\mu \nu_L = \frac{1}{2} \bar{\nu} \gamma^\mu (1 - \gamma^5) \nu \end{aligned}$$

left handed current, or  $V - A$  coupling

From this calculation, it is clear that a study of Drell-Yan cross section for the  $Z_0$  would provide a window to the specific  $V - A$  couplings of the SM [5, 20].

This particular study will also provide for a To build a model, one only has to use the asymptotic freedom of the  $L, Q$  terms and the negative slope of the electromagnetic interaction at high mass scales to make the gauge forces meet. The mass scale at which you

get the couplings to meet is your unification energy.

### *GUTs*

The SM, which has been more or less gospel for decades, agrees with experimental data excellently. The  $SU(3) \times SU(2) \times U(1)$  symmetry group provides all the gauge symmetries needed to describe everything from electromagnetic interactions with photons to the apparent impossibility of free quarks. However, the SM has been labeled inadequate. In spite of its success, the SM does not unify all the forces. The SM also has a number of *a priori* parameters and *ad hoc* features (e.g. heirarchy, left handed charged currents, etc.) [7].

The simplest idea for leptons and quarks, is to put the particles into a larger symmetry group; make  $SU(3) \times SU(2) \times U(1)$  a subgroup of a larger group. One of the most successful schemes involves an  $SU(5)$  representation, which without inputs to the theory, gives fractional quantization of quark charge and even the neutrality of atoms. Typical GUTs unifying electroweak and strong forces attempt to calculate an energy scale at which the coupling strengths of the forces are (hopefully) linearly related.

However, even the  $SU(5)$  representation unification scheme seems inadequate. None of the  $SU(5)$  theories can easily accomodate gravitational interactions. There is a good reason; gravity's mass scale is huge, as the length scale associated with gravity is the Planck length,  $R_{Pl} = 10^{-33}$ cm. That means that the current tools for calculating unification theories cannot bring gravity and the electroweak forces together; the coupling strengths would not converge to the same place in coupling-mass scale space [5].

Furthermore, The  $SU(5)$  representation has been shown to be inconsistent with  $\sin^2(\theta_W)$  and the proton lifetime,  $\tau_p$ . [1, 2]

*Extra gauge bosons from  $E_6$*

Prior to the discovery of the top quark, the  $E_6$  representation was noted to be the next highest anomaly-free gauge group beyond  $SO(10)$ . This led to a large amount of study, and as with many theories, its novelty eventually wore off as the models for the most part allowed the  $b$  quark and  $\tau$  lepton fill in the representation for a “top-less” model (salacious name, if you ask me). As soon as it was generally accepted that the  $b$  and  $\tau$  were members of a third generation, these models were all but abandoned. However, it was shown in the early 80s [7, 8] that the  $E_6$  models might be usable after all. Green and Schwarz showed in 1984 that string theory in 10 dimensions is anomaly-free as long as the gauge group used is  $E_8 \times E'_8$  or  $SO(32)$ .  $SO(32)$  does not give chiral fermions, so it doesn't fit with the SM.  $E_8 \times E'_8$ , on the other hand, can contain the SM in its unaltered form, since its fermions create a chiral representation. To create a field theory, one simply takes the limit of large string tension, and the string excitations are integrated out. The resultant representation is a 10D supergravity coupled to an  $E_8 \times E'_8$  gauge sector. To get to our world, we need to compactify the remaining six dimensions into another manifold. Several different schemes have arisen, since the technical details of orbifold geometry allow for many different compactification topologies [7].

Calabi-Yau compactification with an  $SU(3)$  holonomy takes our  $E_8 \rightarrow SU(3) \times E_6$ . The  $SU(3)$  links spin to the compactified space. The remaining  $E'_8$  only couples to the matter states of the  $E_6$  in gravitational interactions, and may prove to be the SUSY breaking sector not yet seen, and may provide a solution for dark matter. After compactification from 10

to 4, an unbroken  $N = 1$  SUSY is left. Depending on the topology of the compactification scheme, several different rank 5 or 6 subgroups  $S$  are left from the  $E_6$ ,

$$\text{Rank 5 } S = SU(3)_C \times SU(2)_L \times U(1)_Y \times U(1)_\eta$$

$$\text{Rank 6 } S = SU(3)_C \times SU(2)_L \times U(1)^3$$

$$SU(3)_L \times SU(2)^2 \times U(1)^2$$

$$SU(3)^3$$

$$SU(4) \times SU(2) \times U(1)^2$$

$$SU(2) \times U(1) \times G(n, \forall n \geq 2)$$

...

Since  $SU(3)_C \times SU(2)_L \times U(1)_Y$  has rank 4, we clearly have at least one other neutral gauge boson in the rank 5 or 6 cases. It is also clear that further symmetry breaking is needed. One common solution is an effective Higgs field. This does the job nicely, allowing the rank 5 representation to break down into  $U(1)_Y$  as necessary [7].

### Model 1

Perhaps the simplest case is the following breakdown:  $E_6 \rightarrow SU(5) \times U(1) \rightarrow SU(3)_C \times SU(2)_L \times U(1)_Y \times U(1)_\eta$ . Here, the compactification scheme has left a single  $U(1)_\eta$  symmetry. This symmetry leads to a single neutral gauge boson, a  $Z'$ . This single  $Z'$  is one of the most studied cases, because of ease of calculation [7].

## Model 2

### *Rank 5: $Z'$ mixing*

In the rank 5 case,  $E_6 \rightarrow SO(10) \times U(1)$ . The  $U(1)$  may be labelled as  $U(1)_\psi$ , and the  $SO(10)$  may further break down;  $SO(10) \times U(1)_\psi \rightarrow SU(5) \times U(1)_\chi \times U(1)_\psi$ , the new  $U(1)$  being labeled  $U(1)_\chi$ . Now there are *two* extra  $U(1)$  symmetries that can each lead to gauge bosons. These two  $U(1)$ s can form an orthogonal pair of abelian generators, independent of the electric charge. The generators for this symmetry group are:

$$Z'_\psi = \frac{1}{\sqrt{2}} (1 \ 0 \ 0 \ 0 \ 0 \ 0) \quad (19)$$

$$Z'_\chi = \frac{1}{\sqrt{10}} (0 \ 1 \ 1 \ 1 \ 1 \ 1) \quad (20)$$

If at least one of the mass eigenstates of these generators is light enough to be detected, it can be expected that a superposition state of the two may be visible also. An intermediate  $Z'(\theta)$  is defined as an overlap of the two states;  $Z'_1(\theta) = Z'_\chi \cos(\theta) + Z'_\psi \sin(\theta)$ , with  $\theta$  the  $(\chi - \psi)$  mixing angle. Another state is easily defined;  $Z'_2(\theta) = Z'_\chi \cos(\theta) - Z'_\psi \sin \theta$ . These overlap states could be seen easily if the mass of one or both is light enough to allow it in Drell-Yan processes at colliders [8, 7].

## Model 3

### *Three lepton families?: $G_{MSM} \times U(1)_{L_i}$*

Traditionally, the SM has three lepton families;  $e, \mu, \tau$ . These families can each be described by the quantum number  $L_{e,\mu,\tau}$ , the lepton family number. Under minimal standard model, MSM, the interaction lagrangian,  $\mathcal{L}_{int}$  is invariant under the symmetries  $U(1)_{e,\mu,\tau}$ , as

there are no lepton family violating processes observed. A new basis can be defined;  $L_{i=1,2,3}$ .

The rules are as follows:

$$L_1 = L_e - L_\mu \quad (21)$$

$$L_2 = L_e - L_\tau \quad (22)$$

$$L_3 = L_\mu - L_\tau \quad (23)$$

$$[L_i, L_j]_{i \neq j} = 1; i, j \in [1, 2, 3] \quad (24)$$

$$\Psi = \alpha_\xi L_e + \beta_\xi L_\mu + \gamma_\xi L_\tau \quad (25)$$

Where  $\Psi$  is the representation of any lepton,  $\xi \in [1, 2, 3]$ . With this new representation comes a new  $U(1)_{L_{1,2,3}}$  symmetry. The new representation is written  $G_{MSM} \times U(1)_L$ . This means that there is a second neutral gauge boson in addition to the SM  $Z_0$  for each of the new lepton re-defined bases,  $i = 1, 2, 3$ . So, the new  $Z'$ 's are labelled  $Z'_1, Z'_2, Z'_3$  accordingly. If the gauge couplings  $g'_{1,2}$  are small enough, the  $Z'_{1,2}$  could be massless.  $g'_3$  can be set [10] by standard methods for this massless limit to be  $\leq 10^{-24}$ , so there is room for an observable. The massless  $Z'_3$  would couple to the  $\mu(g-2)$ , and thereby imply that the  $g'_3 \leq 10^{-5}$ , making an observable far more difficult since  $\mu(g-2)$  is so well known [9].

## Model 4

*Low Energy effective EW group:  $U(1)_L \neq U(1)_Y$*

Again, compactifying from  $E_8 \times E'_8$  to  $E_6 \times E'_8$ , what remains will become the SM fields and an  $E_8$  “shadow world” with only gravitational interactions, respectively. The  $E_6$  has

room for much variation in gauging schema. As usual, the  $E_6$  fermions are put into a **27**-plet with the usual set of particles;  $u, \bar{u}, d, \bar{d}, e^\pm, \nu_{e,\mu,\tau}, \dots$ . But, not breaking down into the usual groups first gives rise to even more particles; right handed  $\nu$ 's, isosinglet  $-\frac{1}{3}$  charge  $q, \bar{q}$ , 2 lepton isodoublets  $(\nu_E, E^-), (E^+, \bar{\nu}_E)$ , and a neutral isosinglet lepton  $N$ .

A particular maximal subgroup of  $E_6$  is  $SU(3)_C \times SU(3)_L \times SU(3)$ , where the **27** =  $(3, 3, 1)_q + (\bar{3}, 1, \bar{3})_{\bar{q}} + (1, \bar{3}, 3)_l$ . The lepton  $SU(3)$  can break down into an  $SU(2)$  and a  $U(1)$ . However, it is interesting to note that this  $U(1)$  is not the hypercharge of the SM;  $U(1)_L \neq U(1)_Y$ , with  $Q_{EM} = I_{3L} + \frac{Y}{2}$  since otherwise the quark charge would be zero! Since  $SU(3)_L$  must contribute to the electromagnetic charge, the low energy effective electroweak group must be at least  $SU(2)_L \times U(1)_L \times U(1)$ , meaning that there must be at least one extra  $Z'$  in the low energy theory [8].

## Model 5

### *W, Z mixing due to large G subgroup*

In the typical scheme,  $E_6 \rightarrow SU(2) \times U(1) \times G(n)$ , we can have  $W$  and  $Z$  mixing from the new  $G(n)$ . For simplicity, the  $Z$  mixing will be discussed and the extension to the  $W$  follows logically. If the  $G(n)$  has an extra neutral  $Z'$ , the derivation from the extra  $U(1)$  from Model 1 stands. The extension to the  $W$  follows naturally, if the extra  $G(n)$  also has a charged current vector boson.

The compactification from  $E_6$  down to our world can have even more neutral gauge bosons. The  $SO(10)$  symmetry group has rank 6, but the  $SU(5)$  group has rank 5. So, compactifying from  $SO(10) \rightarrow SU(5)$  picks up an extra neutral gauge boson;  $SU(5) \times U(1)_\lambda$ . Likewise,  $E_6$  has one higher rank than  $SO(10)$ , so going from  $E_6 \rightarrow SO(10)$  picks up another neutral gauge boson;  $SO(10) \times U(1)_H$ . The boson that arises from compactifying from  $E_6$

has an index  $H$  because it is an  $Z'_H$ , a Yang-Mills coupling  $Z'$ . This  $Z'$  should show up in Drell-Yan collisions also for  $\sqrt{s} \simeq 1.6 - 2.4\text{TeV}$  [11].

## Model 6

*Another scheme,  $SO(6) \times SO(4)$*

Another superstring-inspired compactification scheme involves the as-of-yet not mentioned  $SO(10) \rightarrow SO(6) \times SO(4)$  breakdown. The thought is that  $SO(6) \sim SU(4)$ .  $SU(4)$  readily breaks down into the required  $SU(3)_C \times U(1)_Y$  group. The remaining  $SO(4) \sim SU(2)_L \times SU(2)_R \rightarrow SU(2)_L \times U(1)_{R_1} \times U(1)_{R_2}$ . Thus, there are now two right handed neutral current bosons,  $Z'_{R_{1,2}}$  in addition to the usual SM  $Z_0$ . The subsequent mixing of the  $Z'$ s and  $Z_0$ s is expected to be detectable. Since there is no restriction on such interactions, it is also expected that the  $W^\pm$  will mix with the heavier of the two  $Z_{R_{1,2}}$ s [12, 7].

## Model 7

*SUSY partners*

It is assumed that the SUSY partners of the SM fermions,  $\tilde{f}$ , could make a large contribution to the  $Z'$  width. If the right and left handed sfermions are degenerate mass states, the resultant production width,  $\Gamma(Z' \rightarrow \tilde{f}_{L,R} \tilde{f}_{L,R})$  would decrease as much as 50%. This would be exceedingly easy to see in the Drell-Yan process at a  $p\bar{p}$  collider [7].

## Charge Asymmetry, Mass limits, $\frac{d\sigma}{dM}$ , and $A_{FB}$

In the previous section, motivation for the search for extra neutral gauge bosons was presented. Several models suppose the existence of the  $Z'$  boson(s), but how do these models'  $Z'$ s become evident in the context of a collider experiment? Each model can give a prediction of either the front-back asymmetry ( $A_{FB}$ ), modified production/decay widths

( $\Gamma$ ), or the mass dependent differential cross section  $\frac{d\sigma}{dM}$  from Drell Yan events in  $p\bar{p}$  colliders. The calculations are highly model-specific, calculations will follow the model number stated previously. The Drell-Yan  $A_{FB}$  and  $\frac{d\sigma}{dM}$  have been measured numerous times in the context of SM verification. However, the high-mass limit of the  $A_{FB}$  and the  $\frac{d\sigma}{dM}$  has been shown recently to have some deviation from the SM prediction [13, 14]. This deviation points to a possible  $Z'$  signal. The several different models' predictions can apply, and determining which model fits the experimental anomaly will be the task for future experimenters.

### *Rank 5 models and their $Z'$ s*

The most obvious production signal for the  $Z'$  at a hadron collider is the typical  $p\bar{p} \rightarrow Z' + (X) \rightarrow l\bar{l} + (X)$ . In the rank 5 scenarios, the only two that are easily studied are the single  $U(1)$  and the  $U(1)_\psi \times U(1)_\chi$ , as in model 1 and 2 respectively.

In model 1, the two states,  $Z'_{1,2}$  can be further broken into a total of four states, for the angle  $\theta = 0, -90^\circ, -\sin^{-1}(\sqrt{\frac{5}{8}}) \simeq -52.24^\circ, -\sin^{-1}(\sqrt{\frac{3}{8}}) \simeq 37.76^\circ$ , typically labelled in literature [7] as models  $\psi, \eta, \chi, I$  respectively. Each model's couplings are different, so the actual figures for the masses of the  $Z'$ s will differ correspondingly. However, generally speaking we can write the lagrangian coupling for these  $Z'$ s and the SM  $Z_0$ ,

$$\mathcal{L} = \dots + \frac{g}{c_W} \left[ (T_3 - \sin^2 \theta_W) Q Z_0 + \left( \frac{5}{3} \sin^2(\theta_W) \right)^{\frac{1}{2}} Q' Z'_{(\psi, \eta, \chi, I)} \right] \quad (26)$$

for  $Q$  being the quantum numbers coupling the  $Z_0$  to its charges.  $Q' \equiv Q_\psi \cos(\theta) + Q_\chi \sin(\theta)$ , in the resulting effective rank 5 model resulting from the two  $Z$ s mixing to form a single state. Assuming no  $W - Z$  mixing,  $M_W = \frac{gv}{2}$ , where  $v^2 = v_1^2 + v_2^2$ . One then writes the  $Z_0 - Z'$  mass matrix:

$$\mathcal{M}^2 = \begin{pmatrix} M_{Z_0}^2 & \delta M^2 \\ \delta M^2 & M_{Z'}^2 \end{pmatrix} \quad (27)$$

$$\frac{\delta M^2}{M_{Z_0}^2} = 2 \left( \frac{5}{3} \sin^2(\theta_W) \right)^{\frac{1}{2}} \frac{1}{v} (Q'_1 v_1^2 - Q'_2 v_2^2) \quad (28)$$

$$\frac{M_{Z'_i}^2}{M_{Z_0}^2} = \frac{20}{3} \sin^2(\theta_W) \frac{1}{v^2} \sum_{i=1}^4 (Q'_i v_i)^2 \quad (29)$$

The mass matrix can be diagonalized with an orthogonal transformation about  $\varphi$  via

$$\begin{pmatrix} Z_1 \\ Z_2 \end{pmatrix} = \begin{pmatrix} \cos(\varphi) & \sin(\varphi) \\ -\sin(\varphi) & \cos(\varphi) \end{pmatrix} \begin{pmatrix} Z_0 \\ Z'_i \end{pmatrix} \quad (30)$$

here, the angle  $2\varphi \equiv \arctan \frac{2\delta M^2}{(M_{Z_0}^2 - M_{Z'_i}^2)}$ , which gives two mass eigenstates,  $M_{1,2}$ . If the constraint is added that  $M_{Z_0} - M_1 \geq 0$ , the  $M_2$  is calculated to be  $\leq 350\text{GeV}$ . Such a signal should be able to be detected from detailed  $\frac{d\sigma}{dM}$  measurements away from the  $Z_0$  pole [7, 14].

### *Rank 6 and other models*

In model 3, the idea of redefining the lepton families was introduced. If the remaining  $U(1)_{L_i}$  is broken spontaneously,  $Z'_i$  get masses via the Higgs mechanism. This implies that we can add a Higgs scalar field  $S_i$  in the SM, but not under local  $U(1)_{L_1}$ . The non-zero vev for  $S_i$  breaks  $U(1)_L$  giving the  $Z'_i$  masses;  $M_{Z'_i} = g'_i \langle S_i \rangle$ . The natural decay mode we would look for is the  $p\bar{p} \rightarrow Z'_{L_i} + (X) \rightarrow l\bar{l} + (X)$ . Since the  $Z'_3$  couples to the  $\mu$  (g-2) strongly, we can toss it out on experimental evidence. So we only have to contend with the  $i = 1, 2$   $Z'_{L_i}$ s. The  $Z'$  interaction lagrangian can be written out for the fermions based on the neutral gauge boson interaction lagrangian;

$$\mathcal{L}_\gamma = eA_\mu (\bar{e}\gamma_\mu e + \bar{\mu}\gamma_\mu\mu + \bar{\tau}\gamma_\mu\tau) \quad (31)$$

$$\mathcal{L}_Z = \frac{g_2}{\sqrt{1-x}} Z_\mu \left[ \left(x - \frac{1}{2}\right) \frac{\mathcal{L}_L}{eA_\mu} + x \frac{\mathcal{L}_R}{eA_\mu} \right] \quad (32)$$

with  $x \equiv \sin^2(\theta_W)$  and  $g_2$  the SM  $SU(2)$  coupling constant. From the prior definitions of our new lepton bases, the new lagrangians are:

$$\mathcal{L}_{Z'_1} = g'_1 Z'_{1\mu} (\bar{e}\gamma_\mu e - \bar{\mu}\gamma_\mu\mu) \quad (33)$$

$$\mathcal{L}_{Z'_2} = g'_2 Z'_{1\mu} (\bar{e}\gamma_\mu e - \bar{\tau}\gamma_\mu\tau) \quad (34)$$

The front back asymmetry is defined as

$$A_{FB} = \int_0^{\frac{\pi}{2}} \frac{d\sigma(\theta) - d\sigma(\pi - \theta)}{\sigma} \quad (35)$$

$$= \frac{3}{4} \left( \frac{G_{LL}^2 + G_{RR}^2 - 2G_{LR}^2}{G_{LL}^2 + G_{RR}^2 + 2G_{LR}^2} \right) \quad (36)$$

$$G_{LL} = \frac{e^2}{s} + \frac{g_2^2}{1-x} \frac{1}{s - M_{Z_0}^2} \left(x - \frac{1}{2}\right)^2 - \frac{g_1'^2}{s - M_{Z'_1}^2} \quad (37)$$

$$G_{RR} = \frac{e^2}{s} + \frac{g_2^2}{1-x} \frac{1}{s - M_{Z_0}^2} x^2 - \frac{g_1'^2}{s - M_{Z'_1}^2} \quad (38)$$

$$G_{LR} = \frac{e^2}{s} + \frac{g_2^2}{1-x} \frac{1}{s - M_{Z_0}^2} x \left(x - \frac{1}{2}\right) - \frac{g_1'^2}{s - M_{Z'_1}^2} \quad (39)$$

for  $s$  the incident 4-momentum squared. Similarly, the cross sections can be defined;

$$R = \frac{\sigma(e^\pm \rightarrow l^\pm)}{\sigma_{QED}(e^\pm \rightarrow l^\pm)} ; [l = \mu, \tau] \quad (40)$$

$$= \frac{s^2}{4e^4} [G_{LL}^2 + G_{RR}^2 + 2G_{LR}^2] \quad (41)$$

$$(42)$$

So, for different values of  $g'_{1,2}$  relative to the SM  $g_2$ , limits can be set on the maximum  $M_{Z'}$ , and the shape of the resultant  $A_{FB}$  expected in Drell Yan  $p\bar{p}$  dilepton interactions [8].

In model 4, only one extra  $Z'$  is expected. In this scenario, the  $SU(3)^3$  breaks down into  $SU(3)_C \times SU(3)_L \times SU(2) \times U(1)$ . This leads to a 3-fold ambiguity over which remains, so we must choose which two leptons of  $\bar{u}, \bar{d}, \bar{h}$  will form the  $SU(2)_L$  doublet we want to see.

We set the following,

$$Q_{EM} = \left( 0 \ 1 \ \frac{-1}{3} \ \frac{-1}{3} \ \frac{-1}{3} \ 1 \ 0 \right) \quad (43)$$

$$= I_{3L} + \frac{1}{2}Y_L + G \quad (44)$$

$$I_{3L} = \left( 0 \ 0 \ 0 \ 0 \ 0 \ \frac{1}{2} \ \frac{-1}{2} \right) \quad (45)$$

$$Y_L = \left( \frac{-1}{\sqrt{3}} \ \frac{-1}{3} \ \frac{-1}{3} \ \frac{-1}{3} \ \frac{1}{3} \ 0 \ 0 \right) \quad (46)$$

Now, we can write the cross section and the width for  $p\bar{p} \rightarrow Z' + (X) \rightarrow l\bar{l} + (X)$ . The cross section per unit rapidity is defined in the following manner:

$$\frac{d\sigma}{dy} = \frac{4\pi^2 x_1 x_2}{3M_{Z'}^3} \sum_{ij} f_i^p(x_1) f_j^{\bar{p}}(x_2) \Gamma_{ij} \quad (47)$$

where  $f$  is the structure function for the labelled hadron,  $x_{1,2}$  are the momentum fractions, and  $\Gamma_{ij}$  is the partial width of the  $Z' \rightarrow \bar{l}$ . Note that the definition of “lepton” here is both  $l$  and  $q$ . The partial width is defined as

$$\Gamma_{(Z' \rightarrow \bar{l})} = G_F \frac{M_{Z_0}^2}{\sqrt{2}} \frac{M_{Z'}}{4\pi} \frac{2\vartheta \sin^2(\theta_W)}{3} \left( [Q_L(l)]^2 + [Q_R(\bar{l})]^2 \right) \quad (48)$$

where the new coupling is given by  $2\vartheta = (g^2 + g'^2)^{\frac{1}{2}} \left(\frac{5}{3}\right)^{\frac{1}{2}} \sin(\theta_W)$ , and the  $Q_{L,R}$  are the quantum numbers corresponding to the charges that the  $Z'$  couples to. From the partial width and cross sections, the  $A_{FB}$  can be calculated directly. Though, in the interest of space, this particular calculation will be omitted. Suffice it to say, the  $A_{FB}$  would give us a window to look at the high-mass behavior of the couplings. The  $\Gamma_{ij}$  has free couplings, so one can fit to the measured  $A_{FB}$ - effectively “tuning” the coupling. For  $2\vartheta = 90^\circ$ , the  $M_{Z'} \geq 300\text{GeV}/c^2$  for  $\sqrt{s} = 2\text{TeV}$ . Similarly, given a coupling of  $2\vartheta = 0^\circ$ ,  $M_{Z'} \geq 200\text{GeV}$  [8, 15]. Thus, given the recent experimental data from CDF [14], further study of the Drell Yan  $A_{FB}$  is certainly warranted.

In model 5,  $W$  and  $Z$  mixing is allowed to occur in an  $SU(2) \times U(1) \times G(n)$  representation. Since we don't see  $W, Z$  mixing in the SM, we need to have the mixing in the extra  $G(n)$ . Writing the mass matrix again, we see

$$\mathcal{M}^2 = \begin{pmatrix} M_{Z_0}^2 & b \\ b & M_{Z_{G(n)}}^2 \end{pmatrix} \quad (49)$$

where the  $M_{Z_{G(n)}}$  is the mass of the new mixing  $Z'$ . The  $b$  is simply an arbitrary “mixing” mass. Two orthogonal states can be generated through a transformation exactly like equation 30. The resulting mass eigenvectors are

$$Z'_1 = Z_0 \cos(\varphi) + Z' \sin(\varphi) \quad (50)$$

$$Z'_2 = -Z_0 \sin(\varphi) + Z' \cos(\varphi) \quad (51)$$

To set constraints on the masses, the couplings can be manipulated, just as in other models. If one makes the supposition  $M_{Z'_1}^2 < M_{Z_0} \leq M_{Z_{G(n)}}^2 \leq M_{Z'_2}^2$ , the following constraint can be formed;

$$\tan^2(\theta) = \frac{M_{Z_0}^2 - M_{Z'_1}^2}{M_{Z'_2}^2 - M_{Z_0}^2} \quad (52)$$

Given the SM  $Z_0 = 93.8\text{GeV}$ , for  $M_{Z'_1} = 91.9\text{GeV}$ , ( $1 \sigma$  below  $Z_0$  at the time of this analysis [11],  $\tan^2(\theta) \Rightarrow 500\text{GeV} \leq M_{Z'} \leq 1\text{TeV}$ . This again would show up in the differential cross section and the  $A_{FB}$ ;

$$\frac{d\sigma}{d\cos(\theta^*)} \propto (L_q^2 L_l^2 + R_q^2 R_l^2) (1 + \cos(\theta^*))^2 + (L_q^2 R_l^2 + R_q^2 L_l^2) (1 - \cos(\theta^*))^2 \quad (53)$$

for  $\theta^*$  the angle between the quark and the lepton [11].

Model 6 incorporated two additional  $Z'$ s. In that formalism, the  $SO(10)$  reduces to  $SU(3)_Q \times SU(2)_L \times U(1)_L \times U(1)_a \times U(1)_b$ . The new lagrangian is then written and parametrized in a new mass matrix;

$$\mathcal{L} = \partial^\mu + i(g_2 T \cdot W^\mu + g_a T_a B_a^\mu + g_b T_b B_b^\mu) ; [SU(5) \times U(1)^2] \quad (54)$$

$$\mathcal{M}^2 = M_0^2 \mu^2 \quad (55)$$

$$M_0 = Z_0 = \frac{1}{2}(g_2^2 + g'^2)^{\frac{1}{2}} \nu_1 ; g' = \left(\frac{3}{5}\right)^{\frac{1}{2}} g_1 \quad (56)$$

This, of course, complicates the diagonalization,

$$\mu^2 = \begin{pmatrix} \cos^2(\theta) & \sin(\theta) \cos(\theta) & \frac{3\hat{g}}{\sqrt{10}} \cos(\theta) \\ -3 \sin(\theta) \cos(\theta) & \sin^2(\theta) & -\frac{3\hat{g}}{\sqrt{10}} \sin(\theta) \\ \frac{3\hat{g}}{\sqrt{10}} \cos(\theta) & -\frac{3\hat{g}}{\sqrt{10}} \sin(\theta) & \hat{g}^2 \left(\frac{9}{10} + \frac{5}{2} \frac{\nu_2^2}{\nu_1^2}\right) \end{pmatrix} \quad (57)$$

with  $\hat{g} \equiv \frac{g_{a,b}}{\sqrt{g_2^2 + g'^2}}$ .

Now the new mass matrix takes shape:

$$\mathcal{M}^2 = \frac{\nu_1^2}{4} \begin{pmatrix} g_2^2 & 0 & -g_2 g_{B-L} \\ 0 & g_R^2 & -g_R g_{B-L} R \\ -g_2 g_{B-L} & g_R g_{B-L} & g_{B-L} \left(\sqrt{\frac{2}{3}} \frac{\nu_2^2}{\nu_1^2}\right) \end{pmatrix} \quad (58)$$

Now, following the standard techniques, we can calculate the contribution to the  $\frac{d\sigma}{dM}$  and the  $A_{FB}$ . The calculation for the Drell Yan production of a  $Z'$  at a FNAL is given by

$$\left. \frac{d\sigma}{dy} \right|_{y=0} (p\bar{p} \rightarrow Z' \rightarrow \mu^+ + \mu^-)_{\sqrt{s}=1.9\text{TeV}} \simeq 7 \times 10^{-37} \text{cm}^2 = 0.7\text{pb} \quad (59)$$

and thus, the cross section is large enough that in the famed upcoming Run2b, we should be able to detect any such  $Z'$  [12].

## Synopsis

Clearly, there is room for beyond SM physics in the high mass limit of both the Drell Yan  $A_{FB}$  and the  $\frac{d\sigma}{dM}$ . Since the cross sections are relatively large, and the signatures will be quite glaringly non-SM, this particular set of tools and models should prove to be an interesting analysis. The plethora of theoretical models supporting non-SM neutral gauge bosons is astonishing. Many models are self-consistent, and do not conflict *per se* with the current data available. Further study will probably unequivocally rule out or support some of the models examined in this paper, as the  $A_{FB}$  and  $\frac{d\sigma}{dM}$  for Drell Yan events should be a good measure of the models' validity.

## 6 Analysis

The framework of the analysis is relatively simple. First mass  $M$  and  $\cos(\theta^*)$  are calculated for each event. From there, two arrays are defined,  $N_+[\Delta M]$ ,  $N_-[\Delta M]$ ; one pair for each descreet mass bin  $\Delta M$ . The sign of  $\cos(\theta^*)$  for each event determines wether  $N_+$  of  $N_-$  is incremented. Thus, a mass indexed list of the number of events whose  $\cos(\theta^*)$  is  $>$  or  $<$  0 as required for Equation 2. At the end, a table is generated displaying the  $N_{\pm}$ s for each associated mass bin. From this table, the  $A_{FB}$  is calculated for each mass bin.

Currently, the statistical uncertainty does not allow more than a few mass bins. However in this nacent study, 4 mass bins have been chosen;  $M \in [50, 75), [75, 90), [90, 105), [105, 200)$ .

Data Type	Mass Bin	Total	$N_+$	$N_-$
Central-Central	$50 \leq M_{ll} < 75$	61	23	38
	$75 \leq M_{ll} < 90$	281	146	135
	$90 \leq M_{ll} < 105$	407	218	189
	$105 \leq M_{ll} < 200$	13	9	4
Central-Plug	$50 \leq M_{ll} < 75$	21	8	13
	$75 \leq M_{ll} < 90$	141	74	67
	$90 \leq M_{ll} < 105$	203	109	94
	$105 \leq M_{ll} < 200$	31	26	5

Table 3: Data for the  $A_{FB}$  measurement after the analysis code has selected electrons and calculated  $\cos(\theta^*)$

Table 3 lists the current data sample broken down by mass with the  $\cos(\theta^*)$  hemisphere numbers. The current electron selection code finds out of nearly  $11pb^{-1}$  [22] of data, 762 CC  $Z$  candidates, and 396 CP  $Z$  candidates. In the early stages of this analysis a naïve estimate for the errors is being used. Namely, the errors associated with the calculation of  $\cos(\theta^*)$  are ignored, in favor of using the simple counting error of  $\delta N_{\pm} = \sqrt{N}$ . This of course ignores any uncertainty on the luminosity, acceptance or efficiency. However for the purposes of this presentation of the study, it will suffice. Thus, Equation 13 becomes rather simple,

$$\delta A_{FB} = \frac{2 \sqrt{(N_+^3 + N_-^3)}}{(N_+ + N_-)^2} \quad (60)$$

which allows uncertainty estimates to be assigned to the data. The data are shown with errors in Table 4 and in Figure 6. There is an interesting caveat implicit in these data. Since the detector acceptances, luminosity and efficiencies are not accounted for, the error bars on the plot shown are artificially small. The estimated detector efficiency, acceptance and luminosity outlined in James' recent CDF note [21] and internal FNAL resources [22], more accurate error estimates are forthcoming. Equation 11 gives a guide to calculating the

corrected  $A_{FB}$  uncertainty estimate, involving many efficiency studies yet to be completed.

Future iterations of this analysis will include corrected uncertainties for the measurements.

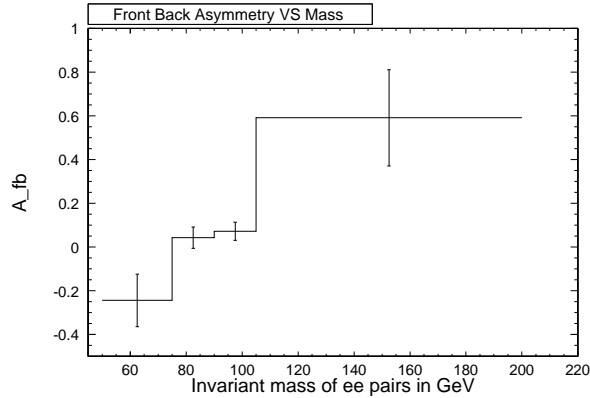


Figure 6:  $A_{FB}$  shown in the four mass bins as a function of the invariant mass of the ee pairs

Mass Bin	$A_{FB}$ Value	Uncertainty $\delta A_{FB}$
$50 \leq M_{ll} < 75$	-0.24	$\pm 0.12$
$75 \leq M_{ll} < 90$	+0.043	$\pm 0.049$
$90 \leq M_{ll} < 105$	+0.72	$\pm 0.041$
$105 \leq M_{ll} < 200$	+0.59	$\pm 0.22$

Table 4:  $A_{FB}$  data with uncorrected uncertainties

## 7 Discussion

Prior studies utilizing  $p\bar{p}$  collider data ?? have included no more than  $110\text{pb}^{-1}$  of data. The current CDF Run II projections suggest that the data sample will grow to more than  $1\text{fb}^{-1}$  by summer 2003 [22]. Figure 7 shows the time integrated luminosity for the current CDF Run II. The study outlined here includes only  $20\text{pb}^{-1}$  of the entire sample. From Equation ??, it is clear that a 10-fold increase in data sample size would decrease the statistical uncertainties by

a factor of 3.16. The data from Affolder, *et al.*, shown in Figure 8 clearly show that a factor of 3.16 decrease in error bars would strengthen the power of the study immensely. Selected

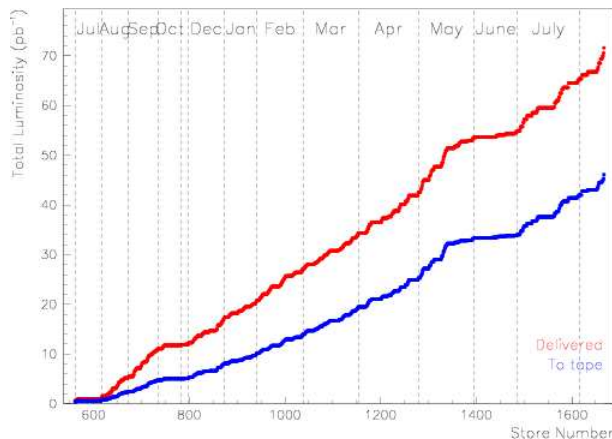


Figure 7: Time integrated luminosity at CDF [22]

beyond-SM models will be studied in the future for this analysis. The  $A_{FB}$  measurement will prove a useful probe of the beyond-SM physics. The high-mass deviation from the SM hinted at above in Figure 8 will be measured with a precision which has never before been utilized. The unique ability of the high energy  $p\bar{p}$  collider to produce high-mass Drell-Yan pairs yields an important tool for examining beyond-SM physics in the  $A_{FB}$ . Hopefully, the continued maturation of this analysis will shed light on some of the beyond-SM models presented herein.

## References

- [1] “New Dimensions at a Millimeter to a Fermi and Superstrings at a Tev”, I. Antoniadis, *et al.*, Phys.Lett. B436 (1998) 257-263

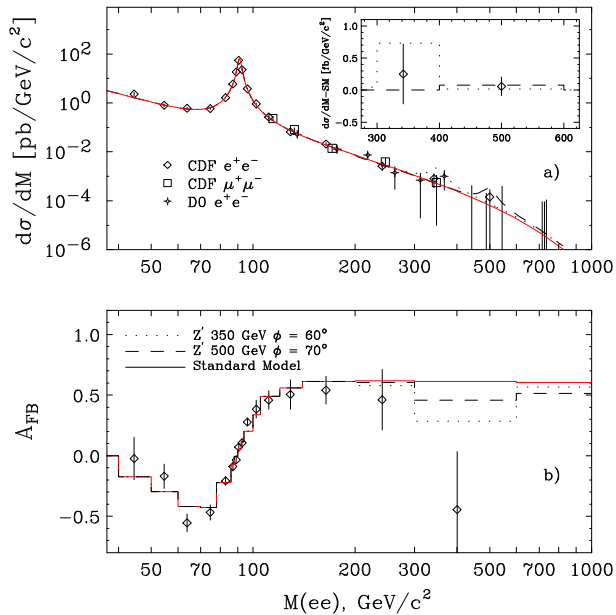


Figure 8:  $A_{FB}$  and  $\frac{d\sigma}{dM}$  for Drell-Yan pairs at CDF by Affolder, *et al.*, [14]

- [2] “Extra dimensions as an alternative to Higgs mechanism?”, M. Shaposhnikov, P. Tinyakov, arXiv:hep-th/0102161
- [3] “Heirarchies without Symmetries from Extra Dimensions”, N. Arkani-Hamed, M. Schmaltz, Phys.Rev., D61, 005-033 (2000).
- [4] “Infinitely Large New Dimensions”, N. Arkani-Hamed, *et al.*, Phys.Rev.Lett., 84, 586-589 (2000).
- [5] “Modern Elementary Particle Physics: The Fundamental Particles and Forces”, G. Kane, Addison-Wesley, 1993.
- [6] “An Introduction to Quantum Field Theory”, M. Peskin, D. Schroeder, Perseus, 1995.
- [7] “Low-energy phenomenology of superstring-inspired  $E_6$  models”, J. Hewett, T. Rizzo, Phys. Rep. 183, 193-381 (1989).

- [8] London, Rosner PRD 34, 1530 (1991).
- [9] X.G. He, G. Joshi, H. Lew, R. Volkas, PRD 43, R22 (1991).
- [10] “Leptons and Quarks”, L. B. Okun, §19.4 North Holland, Amst. (1982).
- [11] P.G. Langacker, Robinett, Rosner, PRD 30, 1470 (1984).
- [12] Robinett, *et al.*, PRD 25, 3036 (1982).
- [13] “Search for New Gauge Bosons in  $p\bar{p}$  Collisions at  $\sqrt{1.8\text{TeV}}$ ”, F. Abe, *et al.*, PRL 68, 1463 (1991).
- [14] “Measurement of  $\frac{d\sigma}{dM}$  and Forward-Backward Charge Asymmetry for High Mass Drell-Yan Pairs”, T. Affolder, *et al.*, PRL 87, 1318 (2001).  
See also CDF note /cdf/anal/electroweak/cdfr/5475 for more in-depth analysis, particularly figure 13.
- [15] E. Eichten, *et al.*, Rev. Mod. Phys. 56, 579 (1984).
- [16] “Determination of  $\sin^2\bar{\theta}_W$  from the Forward-Backward Asymmetry in  $p\bar{p} \rightarrow Z^0 X \rightarrow e^+e^-X$  Interactions at  $\sqrt{1.8\text{TeV}}$ ”, F. Abe, *et al.*, PRL 67, 1502 (1991).
- [17] J. Colins, D. Soper, PRD 16, 2219 (1977).
- [18] “Classical Electrodynamics: Second Edition”, J.D. Jackson. John Wiley & Sons, New York (1975). Especially Chapter 11.
- [19] “Standard Mathematical Tables: Eighteenth Edition”, S.M. Selby. The Chemical Rubber Co. Cleveland, OH (1970).

- [20] “Forward-Backward Charge Asymmetry of Electron Pairs at Large  $Q^2$ ”, J. Berryhill. CDF Note 3489 (unpublished).
- [21] “Studies of Run II High  $P_T$  Muon Data”, E. James, *et al.* CDF Note 5925 (unpublished).
- [22] CDF Luminosity Group. “CDF’s Official Luminosity Web Page”, [http://www-cdf.fnal.gov/internal/people/links/JacoboKonigsberg/lum\\_official\\_page.html](http://www-cdf.fnal.gov/internal/people/links/JacoboKonigsberg/lum_official_page.html) (internal web space).
- [23] CDF Electron Task Force. “Electron Task Force (ETF) Home Page”, [http://www-cdf.fnal.gov/internal/physics/top/r2leptons/etf/etf\\_main.html](http://www-cdf.fnal.gov/internal/physics/top/r2leptons/etf/etf_main.html) (internal web space).

L<sup>A</sup>T<sub>E</sub>X